On-Line Quality Monitoring in Short-Circuit Gas Metal Arc Welding

Results show it is possible to detect changes in weld quality automatically and on-line

BY S. ADOLFSSON, A. BAHRAMI, G. BOLMSJÖ AND I. CLAESSON

ABSTRACT. This paper addresses the problems involved in the automatic monitoring of the weld quality produced by robotized short-arc welding. A simple statistical change detection algorithm for the weld quality, the repeated Sequential Probability Ratio Test (SPRT), was used. The algorithm may similarly be viewed as a cumulative sum (CUSUM) type test, and is well-suited to detecting sudden minor changes in the monitored test statistic. The test statistic is based on the variance of the weld voltage, wherein it will be shown that the variance decreases when the welding process is not operating under optimal conditions. The performance of the algorithm is assessed through the use of experimental data. The results obtained from the algorithm show that it is possible to detect changes in weld quality automatically and on-line.

Introduction

Gas metal arc welding (GMAW) is widely used in various industrial welding applications because it has certain advantages. A high metal deposition rate makes this method attractive for high-quantity applications and well-suited to automatic welding (Ref. 1). There are two stable metal transfer modes in direct current GMAW: 1) short-circuit metal transfer at low arc voltage and 2) spray metal transfer at high voltage. One cycle of the welding voltage waveform for optimum weld parameters corresponds to the transfer of one molten droplet in the short-circuit transfer mode — Fig. 1. Therefore, it is possible to evaluate the stability or regularity of metal transfer using the welding voltage as measured during the welding process (Refs. 2–6).

To assess process stability, standard deviation and different ratios or indices have been calculated for suitable weld parameters, such as arc and short-circuit time, short-circuit rate, short-circuit peak current and mean weld voltage and current (Refs. 2–17).

Monitoring systems for weld parameters such as *ADM III*, *Arc Guard* and *Weldcheck* are commercially available (Refs. 18, 19). They all work in a similar way: voltage, current and other process signals are measured, presented and compared with preset nominal values. An alarm is triggered when any difference from the preset values exceeds a given threshold. It is presently believed that the performance of these systems has not, however, been well-documented.

Experiments have shown that in the short-circuit mode, optimal stability occurs when the short-circuit frequency equals the oscillation frequency of the weld pool (Refs. 5, 6, 20, 21). This corresponds to a maximum in short-circuit frequency. Deviation from the optimal condition leads to a larger probability of spatter, uneven weld bead and other fusion defects. In this case, the welding process is said to operate under non-optimal conditions. Thus, a suitable parameter for the detection of changes in the weld quality is the variance of the amplitude of the weld voltage. This parameter is used to form a test statistic that is fed into a repeated Sequential Probability Ratio Test (SPRT) algorithm (Refs. 17, 22, 23). The algorithm may similarly be viewed as a cumulative sum (CUSUM) type test. The SPRT is optimal in that it minimizes the worst mean delay for detection, given a specified probability for false alarms (Ref. 24). Thus, the algorithm is well-suited to detecting abrupt minor changes in the monitored test parameters (Ref. 22). In addition, storage and computational requirements for the repeated SPRT are moderate, as compared to fixed, sample-sized tests.

KEY WORDS

Algorithm
Cumulative Sum Test
Kullback information
Short-Circuit-GMAW
Step Disturbance
Sequential Probability Radio Test
T-Joint

Welding Technology

Short-Circuit Metal Transfer

The GMAW process employs a consumable wire electrode passing through a copper contact tube — Fig. 2. Electric current supports an arc flowing from the end of the electrode to the workpiece. The electrode is melted by resistive heating and heat from the arc. The region surrounding the weld pool is purged with shield gas to prevent oxidation and contamination of the weld joint (Refs. 2, 25, 26). The advantage of short-circuit welding is that the mean current (thus the average heat input to the workpiece) is lower than in spray arc GMAW (Refs. 11, 19, 27, 28). Due to the smaller heat transfer, short-circuit gas metal arc welding

S. ADOLFSSON is with the Department of Signal Processing, University of Karlskrona/Ronneby and the Department of Production and Materials Engineering, Lund University, Sweden; A. BAHRAMI is with the Technology Center of Kronoberg, Växjö, Sweden, and also Lund University; G. BOLMSJO is with Lund University and I. CLAESSON is with the University of Karlskrono/Ronneby.

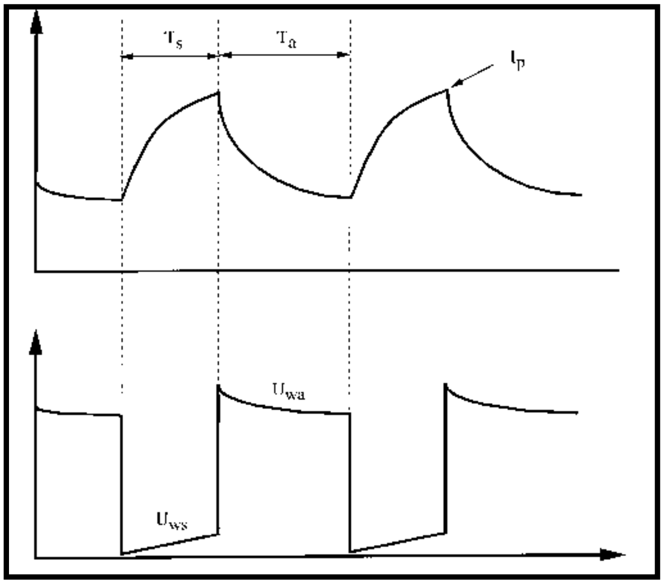

Fig. 1 — *The weld voltage and current during short-circuit welding. The metal transfer is reflected in the weld voltage as almost zero voltage events during short-circuit time T_s. The interval between the short circuits is denoted by short-arc time T_a, while U_{ws} and U_{wa} are the weld voltage during short-circuit and arc time, respectively. I_p is the short-circuit peak current.*

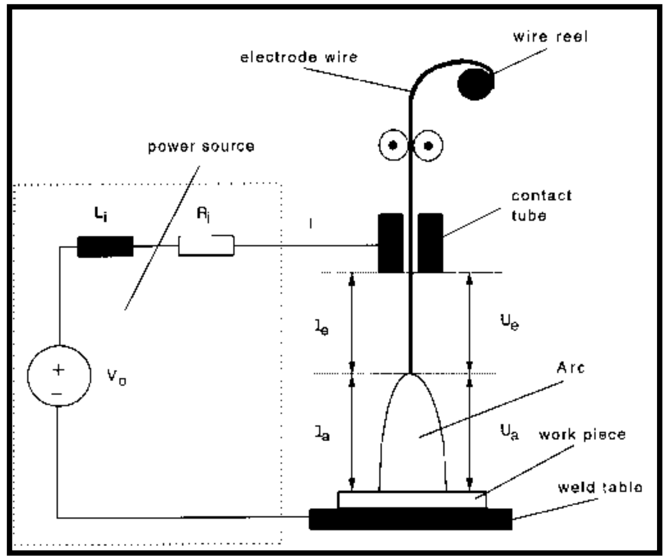

Fig. 2 — *The equipment used in short-arc GMAW. Electric current of the weld process is denoted I. Internal resistance and inductance of the welding source are R_i and L_i, respectively. Resistance of the wire electrode stickout, i.e., the part of the electrode between the contact tube and the arc, is R_e. Length of the electrode stickout and the arc length are l_e and l_a, respectively. Voltage over the wire electrode stickout is U_e. Voltage between the electrode tip and workpiece (the arc voltage) is denoted U_a.*

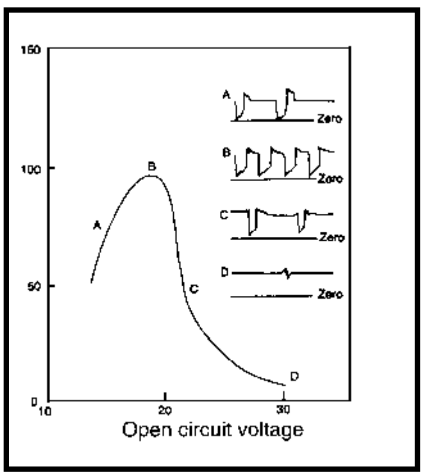

Fig. 3 — *Short-circuit rate for 1.2-mm-diameter wire vs. open-circuit voltage (Ref. 27). Optimal process stability corresponds to the maximum of the curve. Zones A, B, C and D in the curve and oscillograms correspond to stubbing in, short-circuit, globular and spray metal transfer modes, respectively.*

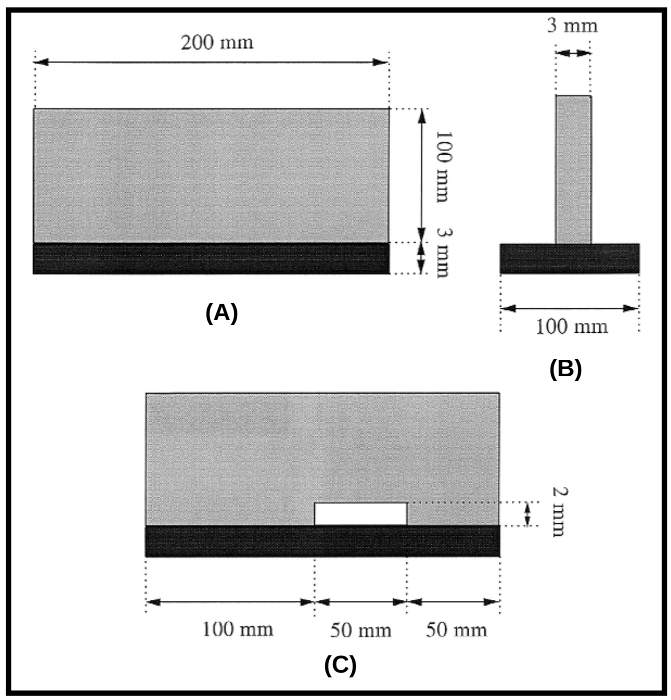

Fig. 4 — *The two steel joints used in the experiments. A — Reference T-joint, front view; B — reference T-joint, side view; C — T-joint with step disturbance, front view.*

(GMAW-S) makes it possible to weld thinner plates than when spray arc GMAW is used.

To limit the heat input to the workpiece, the open circuit voltage is set at a low value compared to that used in spray arc GMAW (Refs. 11, 19, 27). The cycle begins with an arc struck between the electrode wire tip and the workpiece. The wire electrode melts and a small droplet is formed at the electrode tip. This part of the cycle is the arc time, T_a — Fig. 1.

During the short-circuit time, T_s, the voltage will decrease to almost 0 V and the current will increase to its maximum value. At this stage, the arc will extinguish. A droplet is then detached and transferred from the electrode to the weld pool by the force of the surface tension of the weld pool, the gravitational force and electromagnetic pinch force (induced by the current) (Refs. 6, 29). After the droplet is detached from the electrode and transferred to the workpiece, the arc is reestablished and the cycle starts over again.

The weld voltage U_w, arc voltage U_a and the voltage over the wire electrode extension U_e (Ref. 14) are related by

$$U_w = U_a + U_e. \qquad (1)$$

In GMAW-S welding, U_{ws} and U_{wa} denote the weld voltage during the short-circuit time and weld voltage during the arc time, respectively — Figs. 1, 2.

Optimal Process Stability and Welding Conditions

To produce weld joints of uniform weld quality, the welding process should be stable, which will allow metal trans-

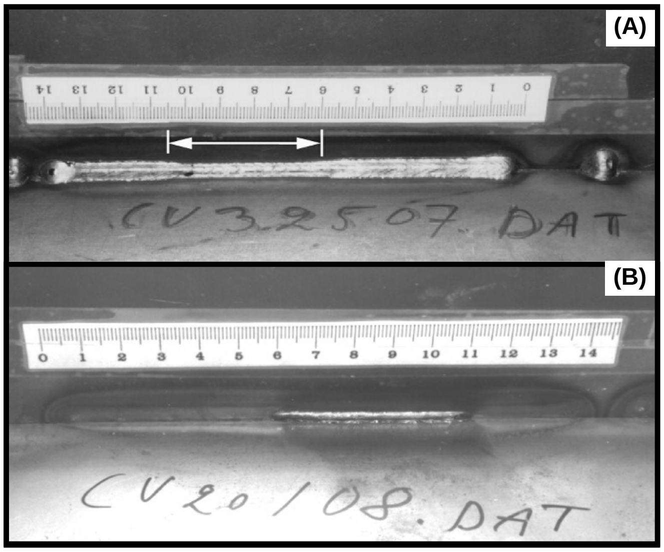

Fig. 5 — T-joint with step disturbance No. 1. Photo of: A — Front; B — rear side of a welded joint. Note that the weld joint at the front of the T-joint in the interval 6–10.5 cm, along the scale (where the weld joint tapers) deviates from normal weld quality, i.e., the size of the leg length and throat dimension is reduced.

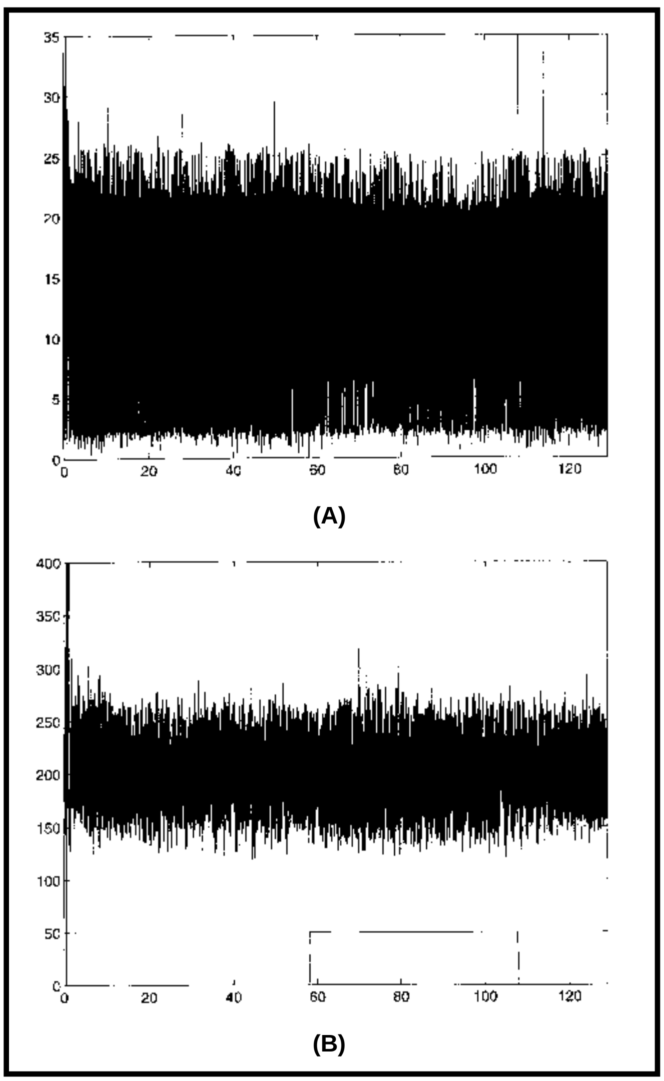

Fig. 6 — T-joint with step disturbance No. 1. A — Measured voltage; B — measured current.

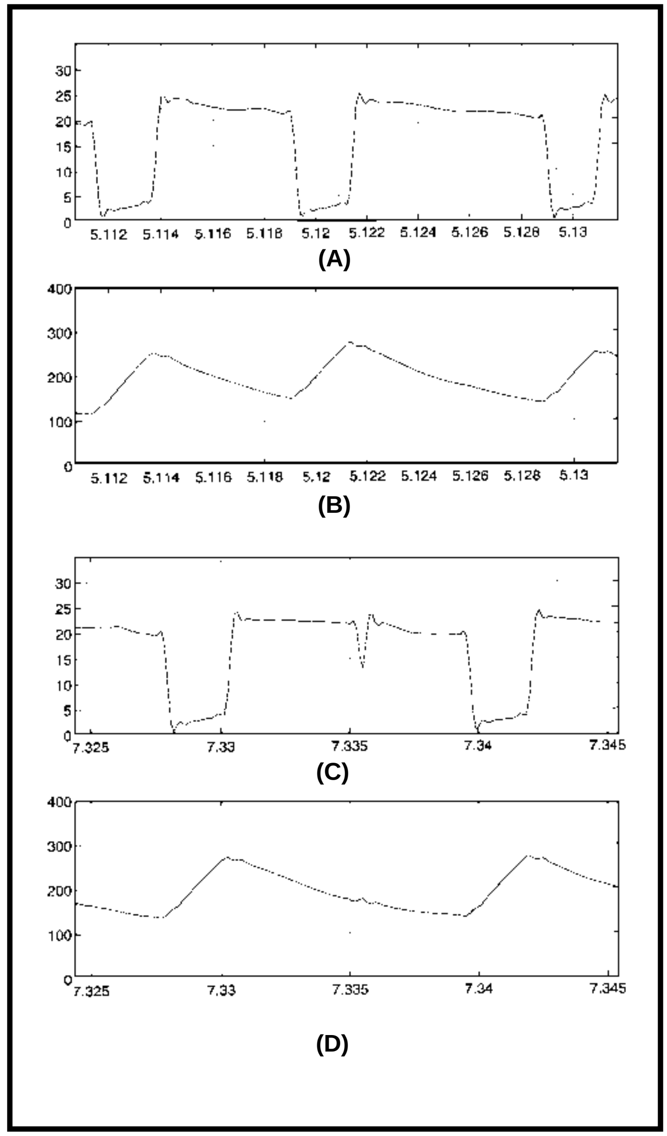

Fig. 7 — Weld voltage and current. Normal weld: A — Measured voltage; B — Measured current. During step disturbance: C — Measured voltage; D — Measured current.

fer from the electrode wire to the workpiece to be as regular as possible. Experiments have shown that in short-circuit mode, optimal process stability occurs when the short-circuit frequency equals the oscillation frequency of the weld pool (Refs. 5, 6, 20, 21). Optimal process stability corresponds to

- a maximum short-circuit rate (Number/s)
- a minimum standard deviation of the short-circuit rate
- a minimum mass transferred per short-circuit
- a minimum spatter loss.

The welding conditions in which optimal process stability occurs are referred to as *optimal welding conditions*. Deviation from the optimal welding condition is assumed to lead to a higher probability of spatter, uneven weld bead and other fusion defects. In this case, the welding process is said to be operating under *non-optimal welding conditions*.

The algorithm discussed in this paper is, however, based on the observation that

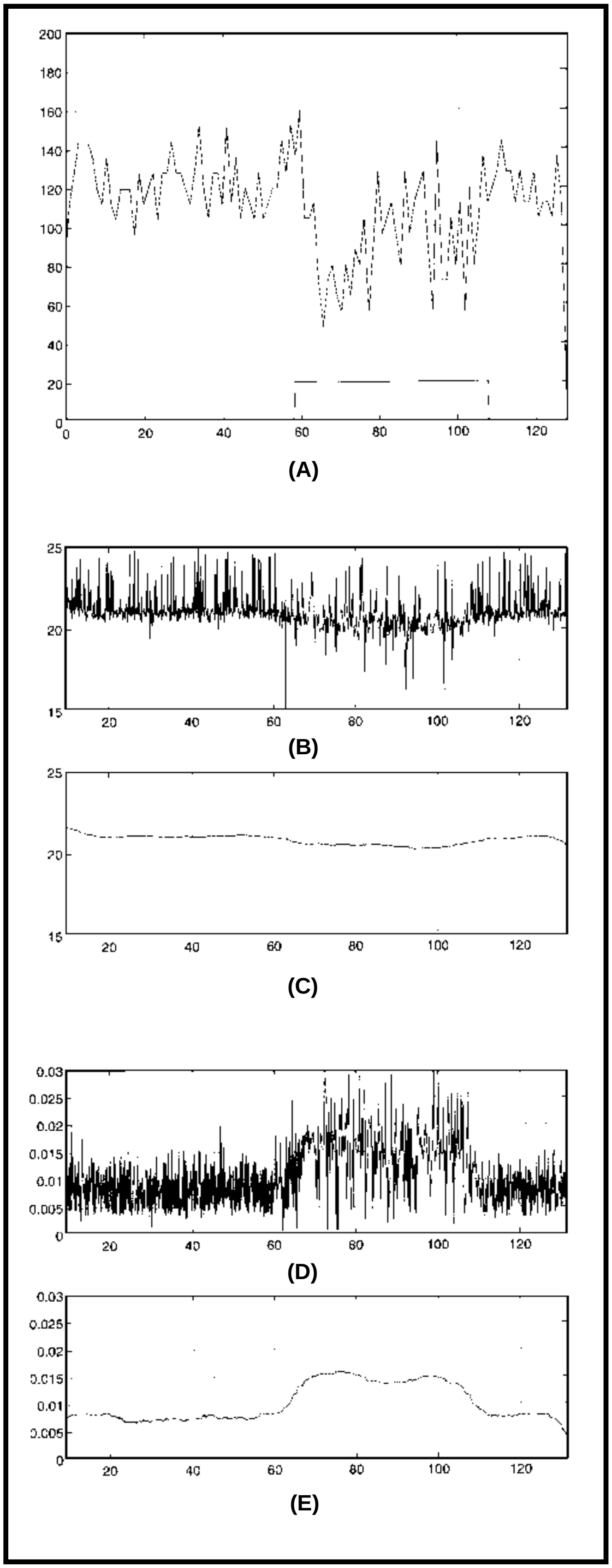

Fig. 8 — T-joint with step disturbance No. 1. A — Measured short-circuit transfer rate; B — estimated mean arc voltage ($\bar{U}_{wa}$); C — median filter of length 100 applied to the estimated mean arc voltage ($\bar{U}_{wa}^{M}$); D — measured arc time (T_a); E — median filter of length 100 applied to the arc time sequence (T_a^M).

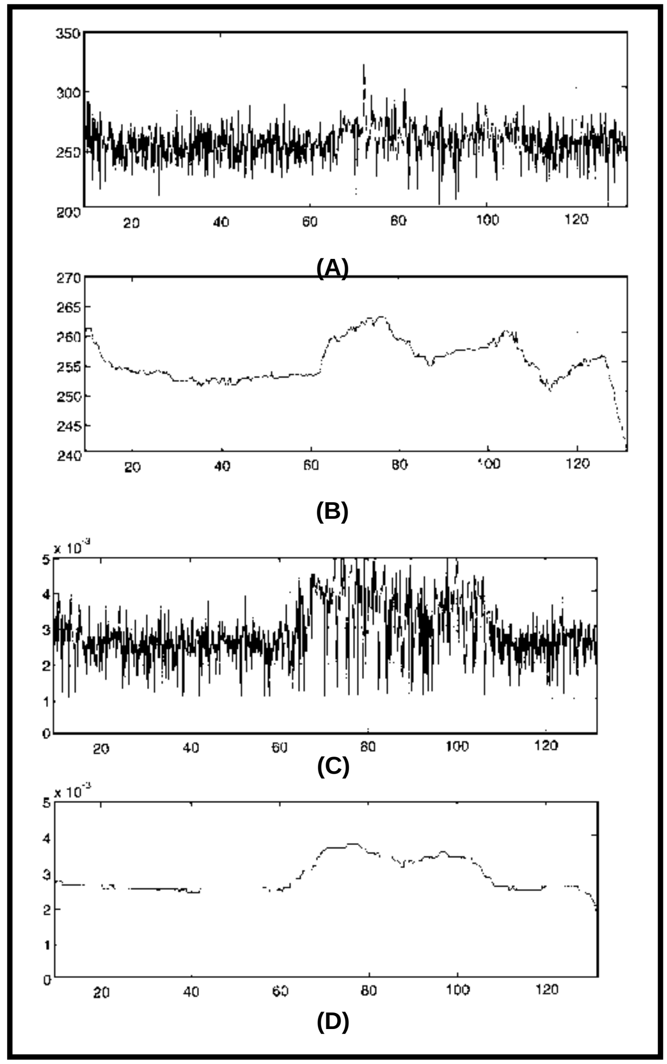

Fig. 9 — T-joint with step disturbance No. 1. A — Measured short-circuit time (T_s); B — median filter of length 100 applied to the estimated short-circuit time in part A (T_s^M); C — measured short-circuit current peak (I_p); D — median filter of length 100 applied to the short-circuit current peak sequence in part C (I_p^M).

the variance of the weld voltage amplitude decreases when the welding process is not operating under optimal conditions, as shown in Fig. 3 (Refs. 11, 13). It will also be shown below that the arc time, short-circuit rate and standard deviation of the short-circuit rate are less robust parameters than the variance of the weld voltage when detecting defective welds.

Experiments

Instrumentation

The experimental setup comprised a welding power source, a Motoman robot carrying a welding torch, a positioner, a welding table and instrumentation for recording weld voltage and current. The work angle of the welding torch was fixed at 45 deg and the travel angle was 0 deg. The distance between the contact tube tip and the plate was 11 mm.

The weld voltage was measured between an electrode applied to the contact tube and a reference electrode screwed into an aluminum plate that served as an insulated welding table (Ref. 14). The current was measured by a current sensor, LEM Module LT 500-S, equipped with a transformer. The sensor was mounted

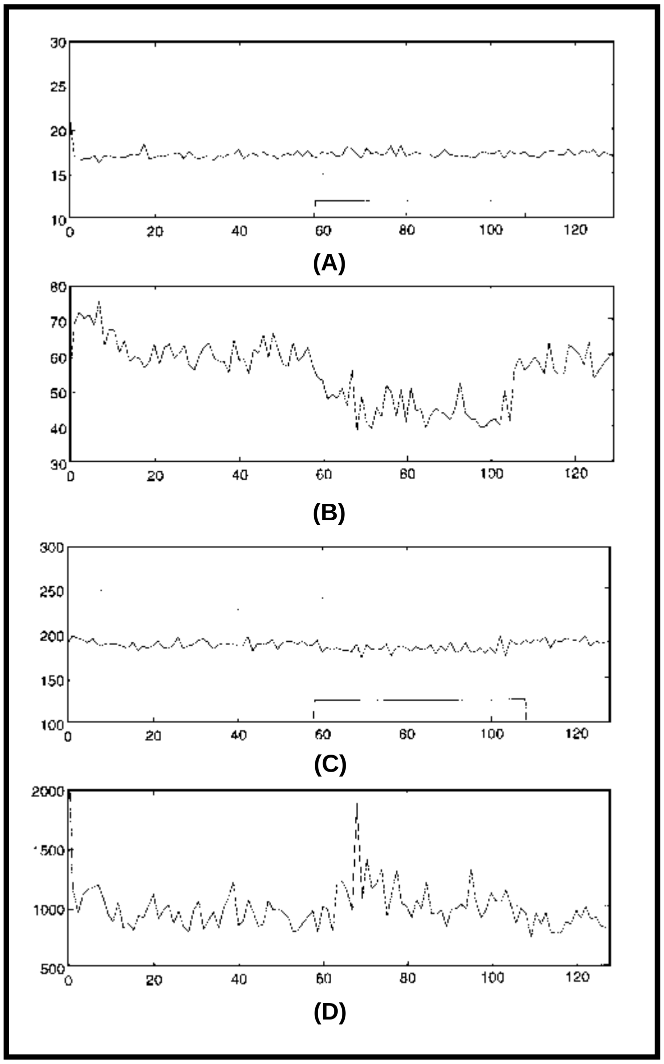

Fig. 10 — *T-joint with step disturbance No. 1. A — Mean of the weld voltage (m[i]); B — estimated variance of weld voltage (y[i]); C — mean of the weld current (mi[i]); D — estimated variance of weld current (yi[i]).*

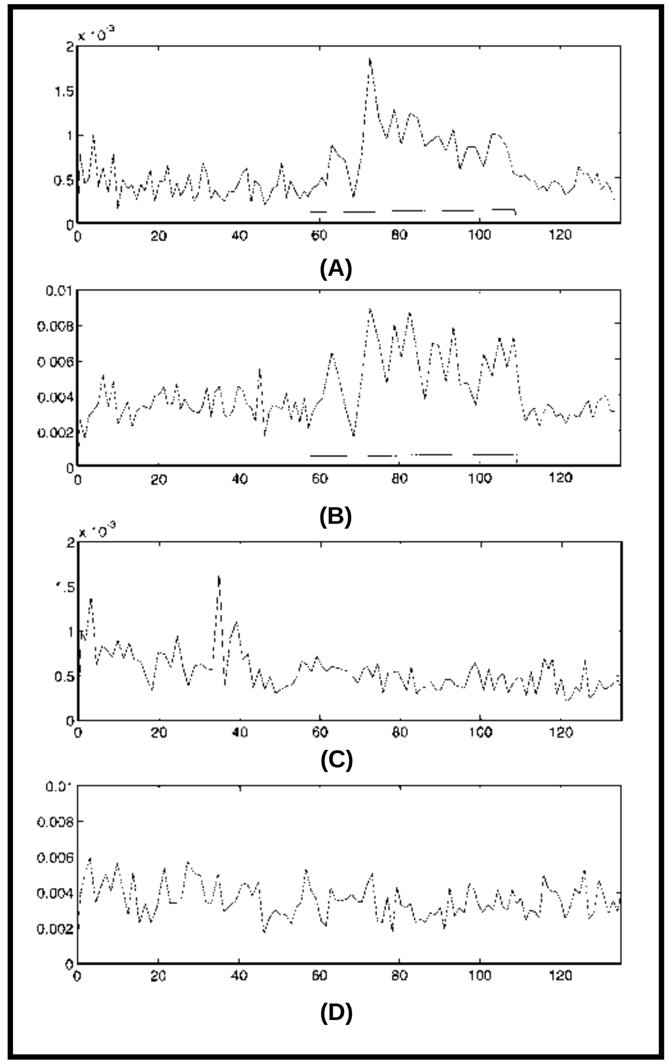

Fig. 11 — *T-joint with step disturbance No. 1. Standard deviation of: A — Short-circuit time (σ_s); B — arc time (σ_a) as a function of position. Reference T-joint. Standard deviation of: C — short circuit time (σ_s); D — arc time (σ_a) as a function of position.*

around the return conductor. The sampling frequency was 8.192 kHz and the total lowpass filter had a cutoff frequency of 3.0 kHz. The data were transferred for permanent storage to a personal computer.

Two different types of commercial welding equipment, the Migatronic BDH S550 and the Kemppi P500, were used in the experiments. The wire feed rate was measured to be approximately 113–120 mm/s and the nominal welding speed was set at 10 mm/s. The welding wire material used in the experiment was ESAB OK 12.51, with a diameter of 1.0 mm. The shielding gas used was Atal: 80%Ar-20%CO_2, with a gas flow rate set at 15 l/min.

Creating Various Welding Conditions

The object of the experiments was to create various welding conditions in a controlled manner, while monitoring the weld voltage and current from the process — Figs. 4–6. Non-optimal welding conditions were created using a T-joint in which gaps had been cut out from the standing plate — Fig. 4. This specimen was denoted "T-joint with step disturbance." With the aid of the step disturbance plate, the welding process passed through non-optimal conditions. A second specimen, a T-joint with the standing plate in perfect contact with the laying plate, was used as a reference. This specimen was used to produce normal welds and was denoted "reference T-joint." During normal welding, the welding process was assumed to be operating under optimal welding conditions.

The specimens comprised two rectangular 200 x 100 x 3-mm plates of SS 1312 mild steel. The dimension of the gap in the T-joint with step disturbance was 2 x 50 mm — Fig. 4C.

A photo of a T-joint with step disturbance is shown in Fig. 5. Note that the weld joint at the front of the T-joint (in the interval 6–10.5 cm along the scale where the weld joint tapers) deviates from normal weld quality, *i.e.*, the size of the leg length and throat dimension is reduced.

Experimental Data Analysis

Time Domain Analysis of Measurement Data

The object of this experiment was to confirm, by examination of the waveform of the weld voltage and current, the assumption that the variance of the weld voltage and weld current decreased when the welding process deviated from the optimal welding conditions. Parameters employed in monitoring short arc

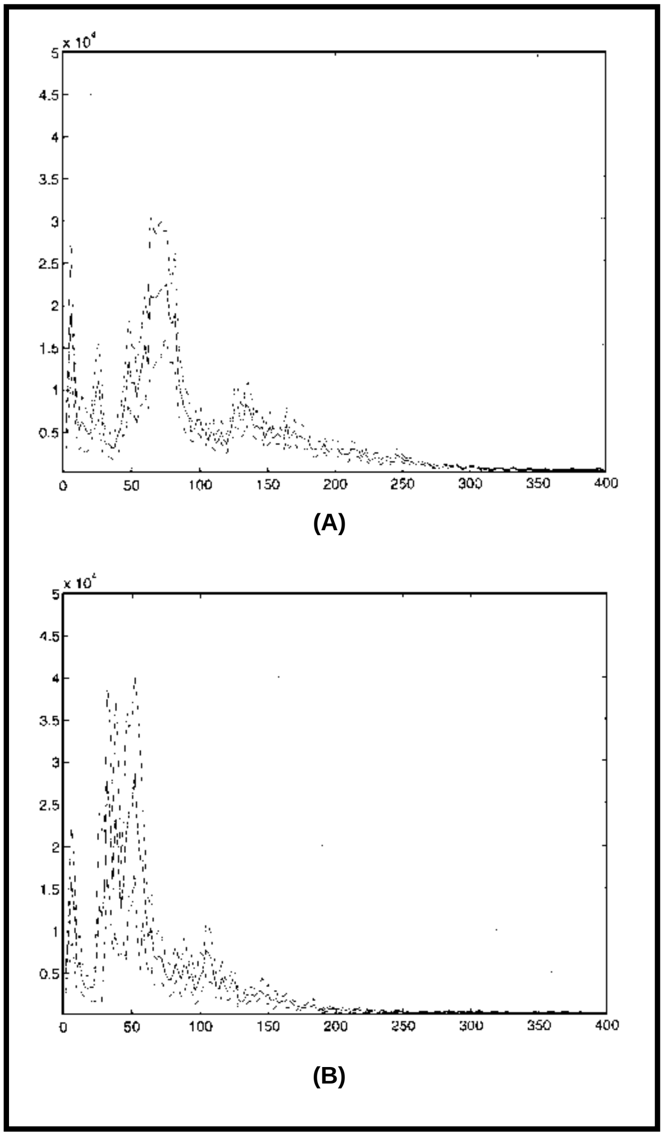

Fig. 12 — Power spectral densities of: A — The weld voltage and weld current from a reference T-joint. Power spectral densities of: B — the weld voltage and weld current during step disturbance. The dotted curve represents 95% confidence limit. Note that the frequency of the spectral maximum peak decreases from about 80 Hz during normal welding to about 50 Hz during step disturbance.

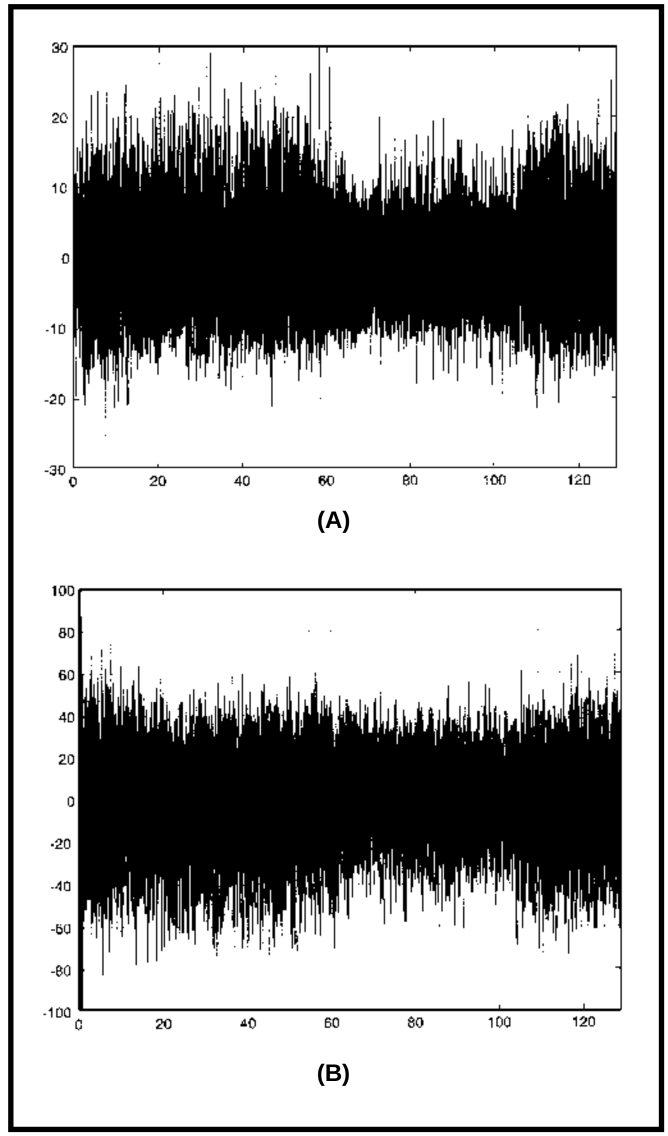

Fig. 13 — Application of high-pass-filter (70 Hz) to: A — Weld voltage; B — current from welding a T-joint with step disturbance. DC and frequency component of the weld voltage and current below 70 Hz is removed and frequency component above 70 Hz is passing through the filter. Note the difference in the waveforms between the non-filtered and the filtered weld voltage and current. (Compare to Fig. 6.)

GMAW were investigated, e.g., arc time, Ta; short-circuit time, Ts; short-circuit peak current, Ip; voltage during arc time, Ua; and voltage during short-circuit time, Us. These variables are key parameters in GMAW and can be estimated whenever the short-circuit time exceeds 1.0 ms — Figs. 8–11. Note that short-term short-circuits, i.e., those that do not exceed 1.0 ms, can result in non-transference of the molten metal (Refs. 27, 30–32).

The figures that illustrate the estimated short-circuit rate are, however, estimated with the number of short-time short-circuits included. This was done to facilitate visual interpretation of the power spectral diagrams — Fig. 12A–D.

To obtain the overall trend for the estimated features, a sliding median filter of length N = 100 was applied to each parameter sequence. The median filter replaced the center value in the window, with the median value of all samples within the window. For N even, xM(k) is the median of

$$x^M(k) = \text{med} \sum_{n=k-N/2}^{k+N/2-1} x[n]. \qquad (2)$$

The output of the median filter is denoted by a superscript *M*, *e.g.*, when a median-filter is applied to the arc time, T_a, the resulting sequence is called T_a^M — Figs. 8–10.

Observation

Two examples of actual recordings of the weld voltages and currents are shown in Fig. 7. Figure 7A and B shows the results of a normal weld; 7C and D show the result of a weld during step disturbance. In Fig. 7A and C, the metal transfers are reflected in the weld voltage as almost zero voltage events of 2 ms. Note that during the step disturbance, the total cycle time, *T*, has increased, as compared with a normal weld. The arc time T_a, short-circuit time T_s and short-circuit peak current I_p have also increased during step disturbance welding, as compared with normal welds, while the short-circuit transfer rate and mean

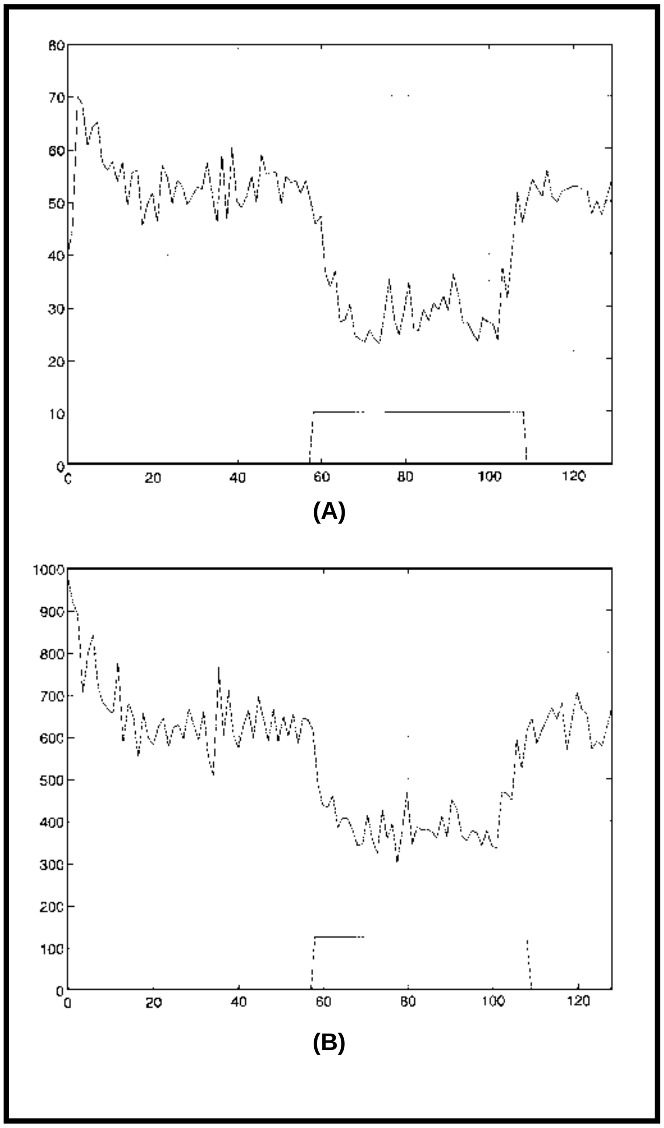

Fig. 14 — Estimated variance of the filtered: A — Weld voltage; B — weld current. Note the similarity in the appearance of the two waveforms. The filtered current shows a decrease in the estimated variance, $yi^f[i]$, while the non-filtered variance estimate of the weld current, yi[i], does not decrease during step disturbance. (Compare to Fig. 10D.)

voltage during arc time, U_{wa}, have decreased — Figs. 8–10.

A possible physical explanation of these phenomena is as follows: When the weld voltage is too low during arc time, the energy in the arc is not sufficient to melt the electrode and form the droplet that is required to complete the weld cycle — Fig. 8B and C. When this happens, an excessive amount of time must be spent in the short-circuit phase to generate the heat necessary to melt the electrode and release the droplet. Consequently, when the short-circuit time increases, the short-circuit peak current also increases — Fig. 9B and D. These figures also suggest that a larger droplet is detached from the electrode for each short-circuit cycle, to compensate for the decreasing short-circuit metal transfer rate during step disturbance to balance the wire melting rate with the wire feed rate.

The weld voltage during arc time is approximately 2 V lower than the open circuit voltage (Ref. 33). The exact value is system dependent. Since the weld voltage during arc time decreases during the step disturbance, the welding process is assumed to be operating in the vicinity of *A*, *i.e.*, the "stubbing-in" metal transfer mode in Fig. 3.

<u>Mean and Variance of the Weld Voltage and Current</u>

As discussed above, the variance of the weld voltage may be a suitable parameter for detection of changes in the weld quality.

The weld voltage is divided into *I* sections, with *N* = 1024 samples in each section. The variance is calculated for each section and given an index, *i*, defined by the position in the sequence. The variance is estimated as follows:

$$y[i] = \frac{1}{N-1} \sum_{n=(i-1)\cdot N}^{i\cdot N} (u[n] - m[i])^2 \qquad \begin{matrix} n = 1, 2, \ldots, N \\ i = 1, 2, \ldots, I \end{matrix} \qquad (3)$$

where $u[n]$ is the weld voltage, N is the number of data points and $m[i]$ is the mean of the weld voltage in section i, calculated as

$$m[i] = \frac{1}{N} \sum_{n=(i-1)\cdot N}^{i\cdot N} u[n] \qquad \begin{matrix} n = 1, 2, \ldots, N \\ i = 1, 2, \ldots, I \end{matrix} \qquad (4)$$

Figures 10A and B show the result of the estimated mean, $m[i]$ and variance, $y[i]$ of the weld voltage amplitude taken from a T-joint with step disturbance. Calculations of $mi[i]$ and $yi[i]$ of the weld current amplitudes are shown in Fig. 10C and D.

From these diagrams, the following conclusions can be drawn:

1) There is a decrease in the estimated variance of the weld voltage and no change in the mean weld voltage during step disturbance — Fig. 10A and B. This supports the assumption that the short-circuit transfer rate has decreased. Since the short-circuit transfer rate has also decreased, non-optimal welding conditions can therefore be assumed — Figs. 3 and 8A.

2) The variance $y[i]$ at the beginning of the welding pass is considerable. This is due to the fact that the process is not stabilized, which leads in turn to the numerous high-voltage transients.

3) Unlike the estimated variance of the weld voltage during step disturbance, no decrease in the estimated variance of weld current $yi[i]$ is observed — Fig. 10C.

<u>Standard Deviation of Short-Circuit Time and Arc Time</u>

The standard deviations of the arc, short-circuit time, short-circuit peak current and short-circuit frequency have often been used as indicators of the stability and regularity of the welding process (Refs. 4–6, 34, 35).

In this study, only the standard deviation of the arc and short-circuit time were calculated since preliminary results showed that standard deviations in peak current and short-circuit frequency yielded no new information. In other words, the behavior of the standard deviation during step disturbance was approximately identical for the four parameters.

The standard deviation was calculated as follows: Short-circuit time and arc time were divided into sections, with ten observations in each section (ten observations of the short-circuit time and arc time corresponded to a weld joint length of approximately 1.0 mm). The standard deviation was then calculated for each section. The results can be seen in Fig. 11.

Spectral Domain Analysis of Measurement Data

Since variance is an AC power estimate (the area below the curve of the power spectral density), spectra from the recordings of normal welding conditions can be compared with spectra of the recordings taken during step disturbance when searching for relevant characteristics (Ref. 36).

The results of the power estimation of

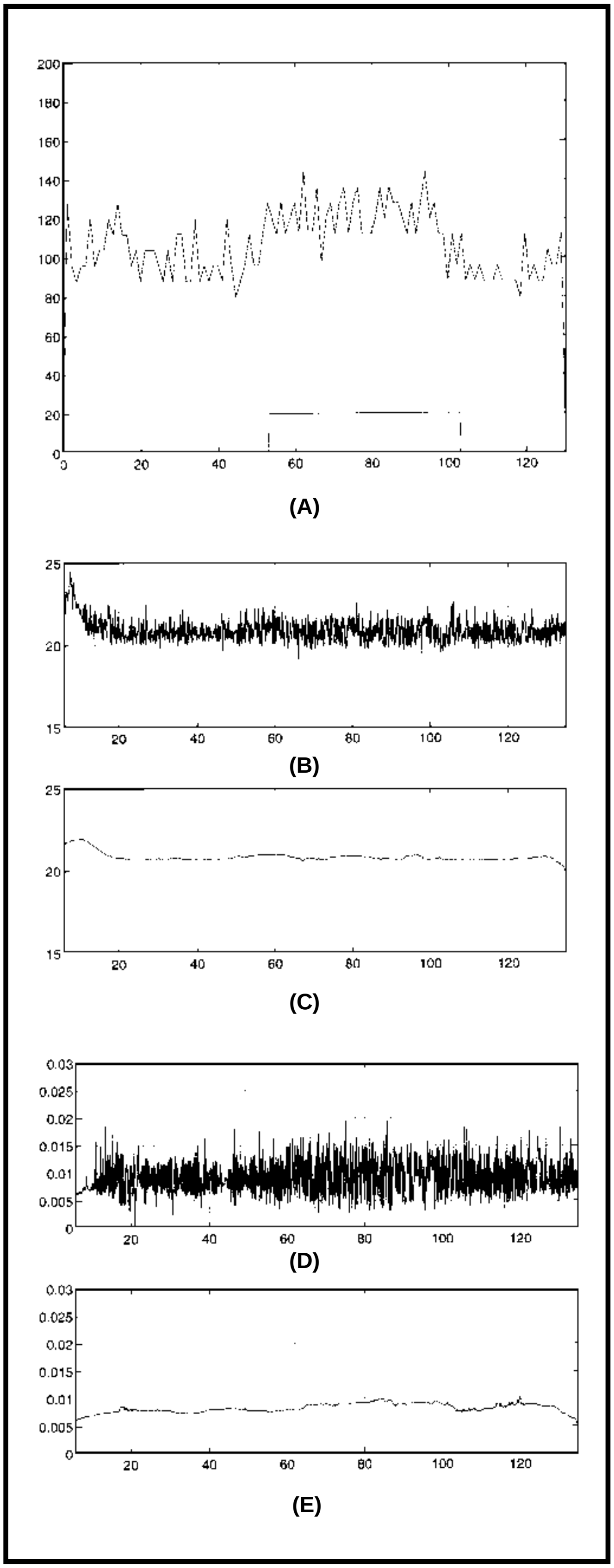

Fig. 15 — T-joint with step disturbance No. 2. A — Measured short-circuit transfer rate; B — estimated mean arc voltage ($\bar{U}_{wa}$); C — median filter of length 100 applied to the estimated mean arc voltage ($\bar{U}_{wa}^{M}$); D — arc time (T_a); E — median filter of length 100 applied to the arc time sequence (T_a^M).

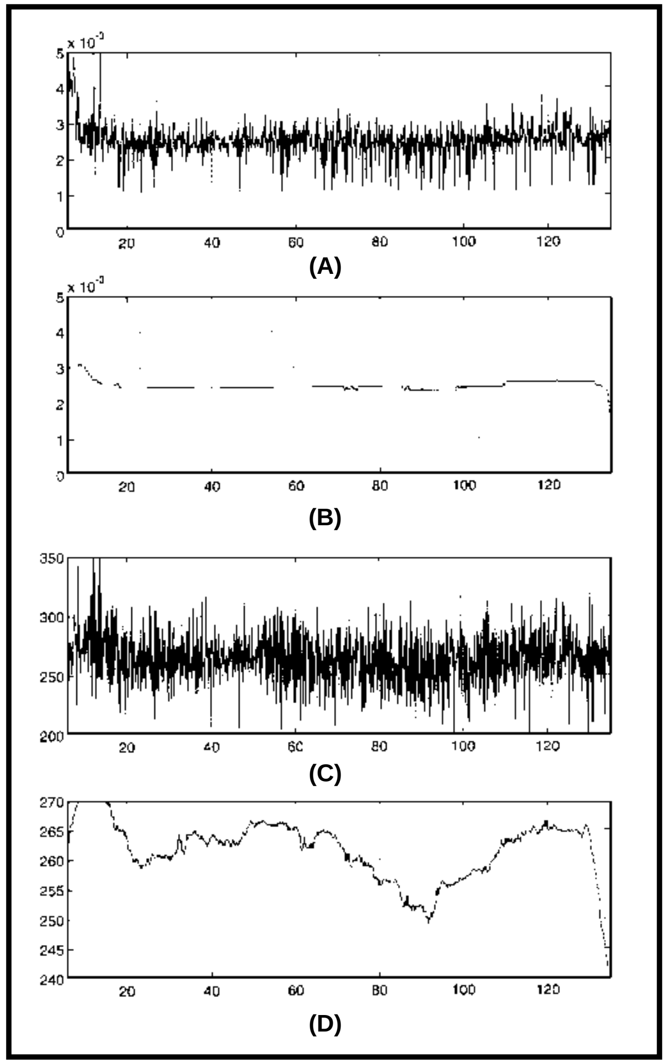

Fig. 16 — T-joint with step disturbance No. 2. A — Measured short-circuit time (T_s); B — median filter of length 100 applied to the estimated short-circuit time in part A (T_s^M); C — measured short-circuit current peak (I_p); D — median filter of length 100 applied to the short-circuit current peak sequence in part C (I_p^M).

the weld voltage and current during both normal welding and step disturbance is shown in Fig. 12A–D. A visual inspection of the four power spectral densities showed that the maximum spectral peak during normal welding was about 80 Hz, compared with the maximum spectral peak during step disturbance, approximately 50 Hz.

The fundamental frequency (80 Hz) of the power spectral density of the weld voltage during normal welding did not seem to be in agreement with the short-circuit transfer rate curve during a normal weld, as shown by a comparison of Figs. 8A and 12A and B. The fundamental frequency (80 Hz) differed from the number of short-circuits (approximately 110/s). The difference may have been due to the fact that short-term short-circuits were included in the total number of short circuits. The maximum spectral peak in Fig. 12A and B represents the true short-circuit rate, where metal is transferred from the electrode tip to the workpiece. The difference between the two results may represent the number of short-term short-circuits/s, estimated as 110 – 80 = 30.

As stated above, a decrease in the variance was reflected in a decrease in the area in the power spectral density.

However, it is not clear in which frequency band the fall in power occurred. Compare Fig. 12A and C. Further investigations must be undertaken.

Filtering the Data

The main difference in the power spectra of the weld voltage and current was the decrease in the frequency of the spectral maximum peak from 80 Hz during normal welding to about 50 Hz during step disturbance. To enhance the difference between normal welds and welds during step disturbance, the weld voltage and current were high-pass-filtered with an elliptic discrete-time filter. The cutoff frequency filter was set at f_2 = 70 Hz.

To avoid any phase distortion of the output, the phase-shift of the filter should be zero. One technique for achieving this is to process the data forward and then backward through the same filter (Ref. 37). is shown in fig. 13A and B. The result of applying the high-pass filter to the weld voltage and weld current in this way.

Variance of Filtered Data

The variances in the amplitude of the high-pass-filtered weld voltage and current may be suitable parameters for detection of changes in the weld quality.

The high-pass-filtered weld voltage and current are divided into *N* sections, with 1024 samples in each section. Denoting the section of the filtered voltage *uf*[*i*] and section of the filtered weld current *cf*[*i*] where *i* = 1, …, *I*, for each section the variance of the weld voltage *yf*[*i*] and current *yif*[*i*] can be calculated.

Figure 14A depicts the result of $y^f[i]$ taken from a T-joint with step disturbance. Note the decrease in the estimated variance of the weld voltage, $y^f[i]$ during step disturbance, indicating non-optimal welding conditions.

The same algorithm was also applied to the filtered weld current to obtain an estimate of the variance in filtered weld current amplitude. The estimated variance for weld current $yi^f[i]$ is shown in Fig. 14B. Note that the filtered current shows a decrease in the estimated variance $yi^f[i]$ while the non-filtered variance estimate of the weld current *yi*[*i*] does *not decrease* during step disturbance. Compare Figs. 10D and 14B.

Note also the similarity in the appearance of the two waveforms between the estimated variance in the filtered weld voltage and the current.

Selected Test Parameter for Monitoring Short Arc GMAW

The observations described above are typical of the welds, though deviations from normal behavior can occur. The normal pattern for a T-joint with step disturbance is shown in Figs. 5–12 as follows:

- a decrease in short-circuit rate and arc voltage
- an increase in arc time, short-circuit time and short-circuit current peak
- no increase or decrease in the mean of the weld voltage and current
- a variance in weld voltage decrease, though there is no variance in weld current
- increase in standard deviation of arc and short-circuit time.

A probable explanation of the above observations is discussed below.

Examples of deviations from the normal pattern for a T-joint with step disturbance are shown in Figs. 15–19 as follows:

- an increase in short-circuit rate and no change in the amplitude of arc voltage
- no increase or decrease in arc time and short-circuit time, but a decrease in short-circuit current peak
- no increase or decrease in the mean of the weld voltage and current
- variance of the weld voltage decreases, while the variance of the weld current remains unchanged
- no increase or decrease in standard deviation of arc and short-circuit time.

The above observations indicate that optimal process stability can also occur during step disturbance (the short-circuit rates increase and the standard deviation of arc and short-circuit time remain constant). Note also that the variance of the weld voltage decreases, despite the fact the short-circuit rates increase during step disturbance. (Compare Figs. 16B and 17A.) Hence, it is still possible to detect step disturbance in the weld joint, even where no optimal process stability has occurred.

The observations in this section suggest that a detection algorithm that uses the variance of the weld voltage or filtered-weld voltage and current shows promise due to its robustness. The variance of the non-filtered weld voltage is chosen as a suitable parameter for the detection of deviations from optimal welding conditions. The high-pass-filtered weld voltage and current are a little more difficult to obtain, and yield no significant improvement in the detection of the relative decrease in the amplitude level of the variance during step disturbance. Figures 10B and 14A confirm this impression.

Fault Detection Algorithm

Test Parameter

The variance of the weld voltage was chosen as the test parameter for detection of changes in weld quality. When the variance of the weld voltage is larger than the variance during normal conditions, spatter or other severe weld defects giving rise to large voltage transients have occurred. When the variance of the weld voltage is less than the variance during normal conditions, the welding process has been disturbed. To avoid any confusion in terms, the variance of the weld voltage, *y*[*i*] is denoted “AC power.”

The AC power is estimated as described in Equation 3 and is shown in Figs. 10 and 17B. Note the decrease in mean of the AC power estimate *y*[*i*] during step disturbance, indicating non-optimal welding conditions.

Algorithm

The algorithm presented below is designed to detect sudden small changes in the monitored parameter.

The AC power sequence **y** = (*y*[0], *y*[1], … *y*[*k*]) is assumed to be identical, independent and Gaussian distributed as follows (Ref. 38):

$$p_\theta(y[i]) = \frac{1}{\sigma_T\sqrt{2\pi}}\, e^{-\frac{(y[i]-\theta)^2}{2\sigma_T^2}} \qquad (5)$$

The welding process is known to operate under either optimal (θ = *m*0) or non-optimal (θ = *m*1) welding conditions where *m*0 > *m*1. Furthermore, it is assumed that prior to *t* = 0, θ = *m*0 and may only change to θ = *m*1 at one of the *i* sampling instants. Consider the problem of testing *k* + 1 hypotheses *H*0, *H*1, … *Hk*, where *Hj* is defined as

$$\begin{aligned} H_j:\ \ &\theta = m_0 \ \text{ for } 0 \le i \le j-1 \\ &\theta = m_1 \ \text{ for } j \le i \le k \end{aligned} \qquad (6)$$

and H_k is the null hypothesis. If the instant of change *j* is fixed, then the sequential probability ration test (SPRT) between H_j and H_k is based on a comparison of the likelihood ratio (Refs. 22, 23, 39)

$$\Lambda_j^k = \sum_{i=j}^{k} \lambda[i] \qquad (7)$$

with

$$\lambda[i] = \ln \frac{p_{m1}(y[i])}{p_{m0}(y[i])} \quad (8)$$

to a threshold h. At the sampling instant k, Λ_j^k is computed. If $\Lambda_j^k \geq h$, then a defect in the weld joint is detected. In the scalar independent case, Λ_j^k is recursively updated as

$$\Lambda_j^{k+1} = \Lambda_j^k + \lambda[k+1]. \quad (9)$$

In the case of a change in the mean value m of an independent Gaussian random sequence $y[i]$ with known variance σ_T^2, the sufficient statistics $\lambda[i]$ are calculated as (Ref. 22)

$$\lambda[i] = \frac{m_0 - m_1}{\sigma_T^2}\left(\frac{m_0 + m_1}{2} - y[i]\right) \quad (10)$$

which is written as

$$\lambda[i] = \frac{\upsilon}{\sigma_T^2}\left(m_0 - y[i] - \frac{\upsilon}{2}\right) \quad (11)$$

where

$$\upsilon = (m_0 - m_1) \quad (12)$$

is the change in magnitude. The SPRT is optimal with respect to the worst mean delay, when the error probability for false alarms goes to zero. The instant of change j is, in fact, unknown. This may, however, be estimated using the maximum likelihood principle (Ref. 40), leading to the decision function and alarm instant

$$g[k] = \max_{0 \leq j \leq k} \Lambda_j^k \quad (13)$$

$$t_a = \min\{k : g[k] \geq h\} \quad (14)$$

The algorithm has been formulated as a set of parallel SPRTs, but may equally be viewed as a repeated SPRT or a cumulative sum (CUSUM) type test. The connection between these alternative points of view has been investigated (Ref. 22). The decision function $g[k]$ introduced in Equation 13 becomes in repeated SPRT formulation

$$g[k] = [g[k-1] + \lambda[k]]^+ \quad (15)$$

and in the Gaussian case

$$g[k] = \left[g[k-1] + \frac{\upsilon}{\sigma_T^2}\left(m_0 - y[k] - \frac{\upsilon}{2}\right)\right]^+ \quad (16)$$

where $(x)^+ = \sup(0, x)$. The alarm threshold h is chosen by a tradeoff between worst mean delay time for detection τ and false alarm probability α. The CUSUM algorithm (Ref. 24) is optimal when α goes to zero:

$$\tau \sim \frac{\ln \alpha^{-1}}{K(m_1, m_0)} \quad \text{when} \quad \alpha \to 0 \quad (17)$$

where

$$K(m_1, m_0) = E_{m_1}\left[\ln \frac{p_{m_1}(y[i])}{p_{m_0}(y[i])}\right] \quad (18)$$

is the Kullback information. In the Gaussian case, the Kullback information is

$$K(m_1, m_0) = \frac{(m_1 - m_0)^2}{2 \cdot \sigma_T^2}. \quad (19)$$

Due to Wald's equality, the probability of false alarms α and the alarm threshold h satisfies following equation:

$$\alpha = e^{-h} \quad (20)$$

when the probability of non-detection goes to zero. The alarm threshold h is therefore easy to obtain for fixed α (Ref. 41). The complete fault detection algorithm may be summarized as follows:

For each section k of 1024 data samples:

1) calculate AC power $y[k]$
2) calculate $g[k] = [g[k-1] + \lambda[k]]$
3) **if** $g[k] \leq 0$ **then** $g[k] = 0$
4) **if** $g[k] \geq h$ **then** set *Alarm.*

Estimation of the Mean and Variance of the AC Power Parameter

The AC power of weld voltage $y[i]$ in Equation 10 is assumed to be identical, independent and Gaussian-distributed, with a mean value m_0 and m_1 under normal and fault welding conditions, respectively. The variance σ_T^2 of the AC power is assumed to be constant, during both normal weld and step disturbance. However, the mean and variance of the AC power are not known and must, therefore, be estimated. Since there are both within-record variations (see Fig. 21C) and between-record variations of the AC power (probably due to slightly different welding conditions occurring during the experiments when welding the different T-joints), the between-record variations are incorporated into the total variance σ_T^2 — Fig. 20.

To estimate the mean value of the AC power factor, the between- and within-record variance from five experiments (each with 32 observations originating from weld voltages recorded during normal conditions and welds during step disturbance) was used. The process model and estimation procedure of the mean, within-record variations, between-record variations and total variance are described in Ref. 17. The results are given in Table 1. For this data, the mean for normal welds is $\hat{m}_0 = 56.60$ and during step disturbance, $\hat{m}_1 = 47.56$. The estimated variances between record are $\hat{\sigma}_R^2 = 0.66$ and $\hat{\sigma}_R^2 = 6.19$, respectively. The estimated variance within the record for a normal weld is $\hat{\sigma}_I^2 = 6.26$ and $\hat{\sigma}_I^2 = 8.84$ during step disturbance. The total variance for the data is $\hat{\sigma}_T^2 = 6.92$ and $\hat{\sigma}_T^2 = 14.75$, respectively.

In the experiment, the total variance σ_T^2 was set at 6.92. Due to an underestimation of the total variance during the step disturbance, the worst mean delay time for detection τ will increase (Refs. 42, 43).

Tuning

In the proposed algorithm, the only tuning parameter is the threshold h (Table 2). Using Equation 20, we computed the worst mean delay for detection τ and chose a false alarm probability α. These may then be used to determine a relevant alarm threshold, h.

If the false alarm probability α is set at 10^{-6} and assuming that the AC power sequence $y[i]$ is Gaussian and statistically independent, the alarm threshold h is calculated to be $h = 13.8$. The reverse arrangement and the χ^2 test was applied to the AC power to test whether or not the AC power was Gaussian and statistically independent (Ref. 44). The outcome of these tests — not included in this paper — shows the AC power is likely to be statistically independent, but non-Gaussian during both normal and step disturbance welding (Ref. 17). Since the AC power sequence $y[i]$ cannot be assumed to be Gaussian, the alarm threshold h is set at 16 to maintain the false alarm probability, $\alpha \geq 10^{-6}$. In real industrial applications, it is recommended that the welder in charge has the option of changing the alarm threshold in accordance with the type of welding mode and application.

Test of the Repeated SPRT Algorithm

The recursive SPRT algorithm was tested on 31 specimens. A total of 15 experiments were conducted for reference

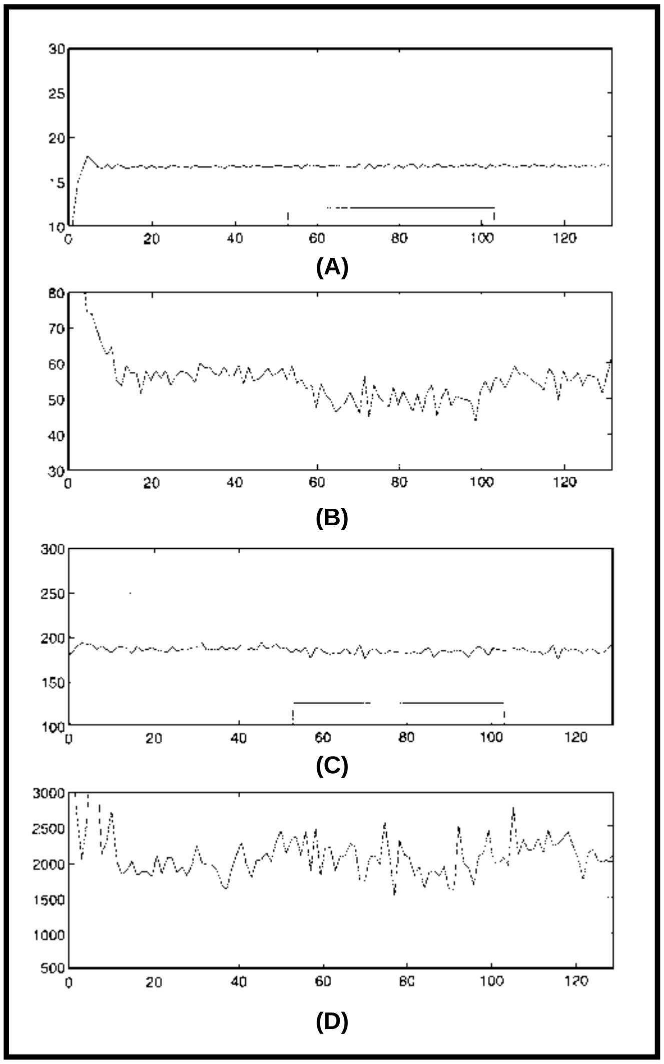

Fig. 17 — T-joint with step disturbance No. 2. A — Mean of the weld voltage (m[i]); B — estimated variance of the weld voltage (y[i]); C — mean of the weld current (mi[i]); D — estimated variance of the weld current (yi[i]).

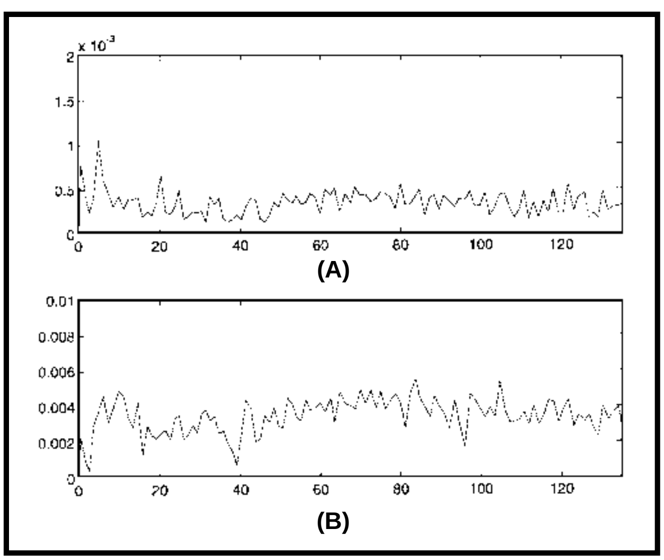

Fig. 18 — T-joint with step disturbance No. 2. Standard deviation of: A — Short-circuit time (σ_s); B — arc time (σ_a) as a function of position.

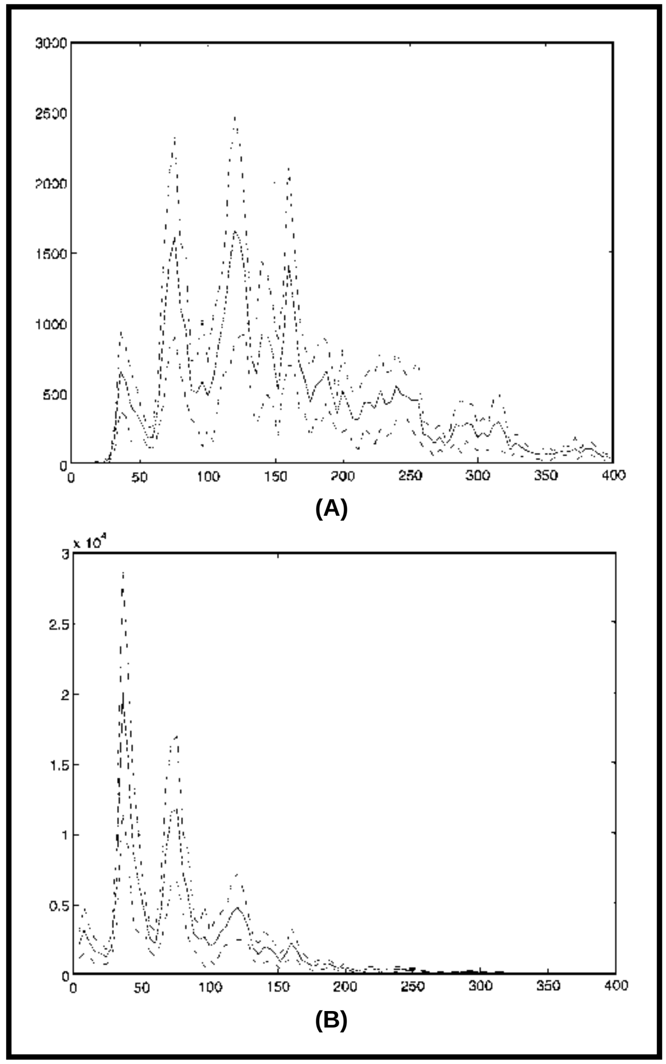

Fig. 19 — T-joint with step disturbance No. 2. Power spectral densities of: A — The weld voltage; B — weld current during step disturbance. The dotted curve represents the 95% confidence limit.

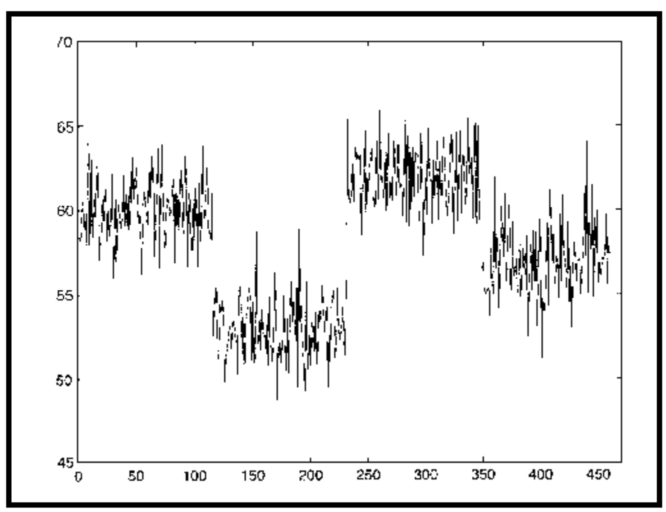

Fig. 20 — The between-record variation of the AC power σ_R^2. This variation is probably due to slightly different welding conditions between the experiments, while the within-record variation σ_f^2 is associated with fluctuations along the weld joint during an experiment. The between-record variation is exaggerated in the diagram for illustrative purposes.

Table 1 — Parameter Estimates During Normal Welds and During Step Disturbance

		Estimated Parameters	
		During Normal Weld	During Step Disturbance
$\hat{\sigma}_I^2$	Estimated within-record variance	6.26	8.84
$\hat{\sigma}_R^2$	Estimated between-record variance	0.66	5.91
$\hat{\sigma}_T^2$	Estimated total variance	6.92	14.75
$\hat{m}$	Estimated overall mean	56.60	47.56

Table 2 — Design Parameters Selected for the Fault Detection Algorithm for Two Different Values of the Change Magnitude, υ = 9 and υ = 2.63, Respectively (Welding Speed is Set at 10 mm/s)

		Design Parameters	
		Test 1	Test 2
υ	Magnitude of change	9	2.63
h	Alarm threshold	16	16
α	False alarm probability	10^{-6}	10^{-6}
h	Alarm threshold	16	16
σ_T^2	Total variance	6.92	6.92
m_0	Mean during normal condition	56.60	56.60
m_1	Mean during non-optimal condition	47.56	53.97

Table 3 — The Experimental Results of Test 1 of the SPRT Algorithm (Magnitude of Change υ, is set at 9 and Welding Speed is Set at 10 mm/s)

	Results	
Type of T-Joint	Reference	Step
Number of specimens	15	16
Detection	0	12
Non-detection	0	4
False alarm	0	0

Table 4 — The Experimental Results of Test 2 of the SPRT Algorithm (Magnitude of Change υ is set at 2.63 and Welding Speed is Set at 10 mm/s)

	Results	
Type of T-Joint	Reference	Step
Number of specimens	15	16
Detection	0	15
Non-detection	0	1
False alarm	0	0

T-joints and 16 experiments were conducted for T-joints with step disturbance. The recording time of the measured signals was 15 s.

The test was designed as follows: When the alarm turns on and there is a step disturbance, the test results in a detection. If the alarm turns on and there is no step disturbance, the result is a false alarm.

Two different changes in magnitude, u = m0 – m1 and u = 1/2sT, were used. The choice of u was dictated by the experimental results in Table 1. The first choice of u is the estimated change in-magnitude; the second choice is the minimum change in magnitude. The minimum change in magnitude is bound to be positive. It is known, however, that the SPRT algorithm is quicker at detecting a magnitude of change between about 1/2sT and 3/2sT from the target value m0, as reflected in the Shewhart chart (Refs. 22, 39, 45).

Since the welding process was not working under optimal welding conditions at the start and end of the welding pass, the alarm was inhibited during the first and last centimeter of the welding pass.

Test Results

The results of the test shown in Tables 3 and 4 indicate that it is possible to detect changes in the weld quality automatically and on-line. To illustrate the results of the data, the test result for a T-joint with a step disturbance is shown in Figs. 21 and 22.

Discussion

All the tests showed consistent results: during a step disturbance, the AC power of the weld voltage decreased. In the experiments, the decrease in the AC power during step disturbance welding was the same for the two different brands of welding equipment used in the experiments. It is likely, therefore, that other equipment of different brands will also exhibit the same behavior. A suitable change in magnitude u and target value m0 must be adjusted for each piece of equipment and for each type of welding.

The proposed SPRT algorithm was designed to detect sudden changes in the average level of the AC power. Four-step disturbances were not detected, however, when the change in magnitude υ was set at 9. These non-detected step disturbances occurred on the same day. A special physical cause could not be found to account for this variation; therefore, these records cannot be excluded from the tests. A probable explanation is that the experimental conditions on the day in question were not identical to the other three. Nevertheless, the recordings from that day all show a decrease in AC power during step disturbance, but the AC power is unusually large — both before as well as during step disturbance. (Compare Figs. 21C and 23.) Since the minimum value that the SPRT algorithm can detect is $m_0 - \upsilon/2$ and the AC power value during step disturbance is above this critical value, these two factors combined explain the lack of detection of the step disturbance.

In industrial welding applications, it is sometimes necessary to weld with mixed-mode transfer to increase the welding speed, thereby increasing productivity. The mix-mode transfer, which contains a mixture of short-circuiting, globular and spray transfer, is related to a working point in the vicinity of C in Fig. 3. In this case, it is relevant to use two SPRT algorithms together: the first for detecting an increase in the mean of the AC power, and the second for detecting a decrease in the mean of the AC power. A new target value m_0, which corresponds to the new working point, must be estimated together with a robust tuning of the minimum magnitude of change in terms of the Kullback information and of

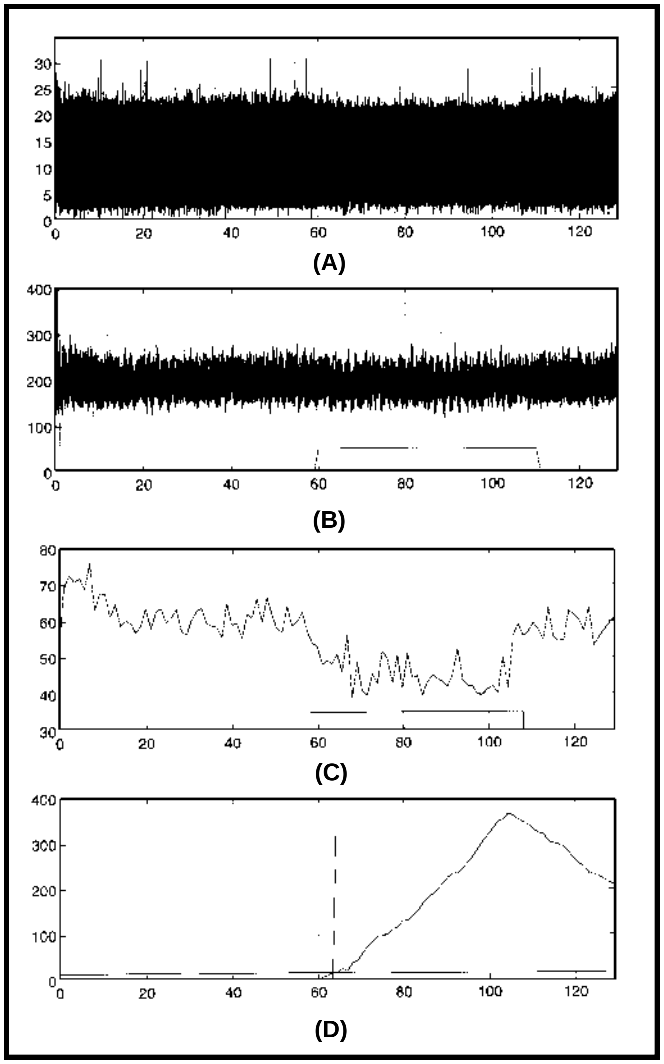

Fig. 21 — Illustration of the detection of step disturbance No. 1. A — Measured weld voltage; B — weld current; C — the corresponding AC power y[i] and the actual position of the step disturbance; D — the behavior of the decision function g[i] and Alarm time. The Alarm time is indicated by a vertical line in the figure. The magnitude of change is set at 9.2 and the welding speed at 10 mm/s.

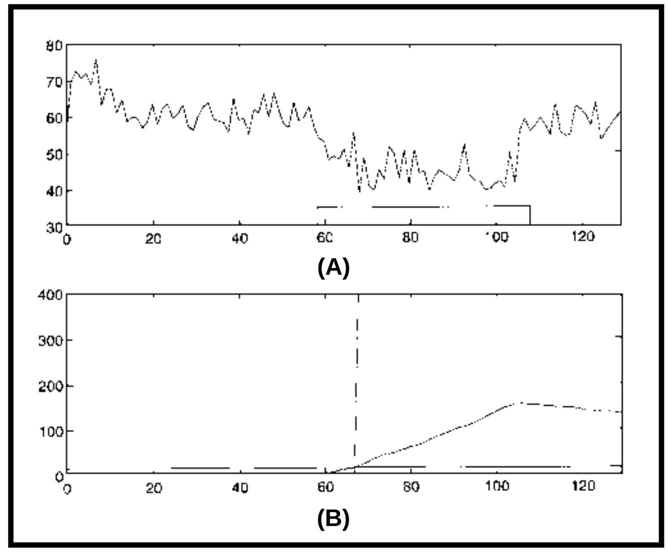

Fig. 22 — T-joint with step disturbance No. 1. A — The AC power y[i] and the actual position of the step disturbance; B — the behavior of the decision function g[i] and Alarm time. The Alarm time is indicated by a vertical line in the figure. The magnitude of change is set at 2.63 and the welding speed is set at 10 mm/s. (Compare with Figs. 21C and D.)

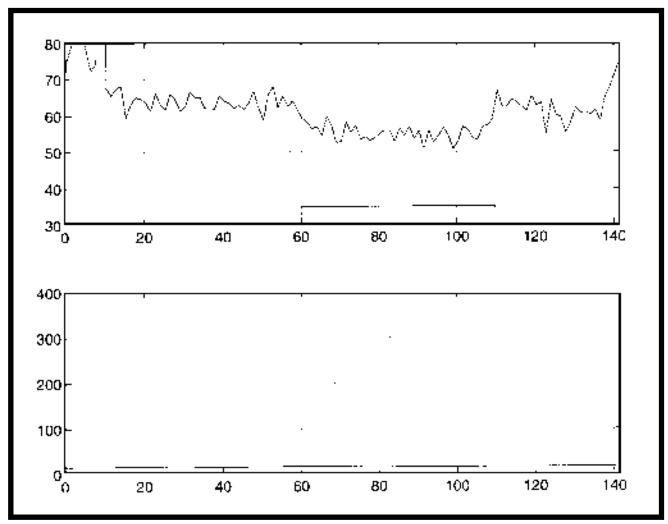

Fig. 23 — The unusually large AC power value before and during step disturbance as compared with a typical T-joint with step disturbance. (Compare with Fig. 21C.) As a consequence of the large AC value during step disturbance, no alarm is indicated in the diagram.

the threshold. The task of the SPRT algorithm is, therefore, to detect when the welding process deviates from the working point.

The decrease in the maximum of the short-circuit frequency during step disturbance may be physically explained by the oscillation behavior of the weld pool as follows: As the oscillation frequency of the weld pool decreases with increasing weld pool width, the maximum short-circuit frequency must also decrease (Refs. 6, 20, 21). However, this explanation is not confirmed by experimental data. The photo of the T-joint in Fig. 5 shows that during step disturbance, the weld joint tapers. Consequently, the short-circuit frequency should increase instead of decrease.

In some cases, the AC power presents large transients in waveform behavior — Fig. 24. A closer examination of the weld joint showed that a severe defect or spatter was generated at the corresponding position on the weld joint. At the point when the molten electrode tip was in contact with the workpiece, a small neck between the electrode and the weld pool developed, due to the surface tension. As a result of this small neck, the current density increased. When the current density in the neck becomes too large, an explosion occurs and a droplet forms. This explosion of the metal bridge gives rise to the high-voltage transients. In this case, the two-sided detection algorithm also seems to be a suitable means of detecting spatter and other severe defects.

To improve the performance of the proposed detection algorithm, other parameters such as short-circuit time and arc time can be incorporated into a composite SPRT detection algorithm (Ref. 22). The difficulty with the composite SPRT detection algorithm is that it gives no indication as to which parameter or parameters are causing the problem. This can be dealt with by using an SPRT algorithm for each parameter, which mentors and simply takes action as soon as the first alarm signal occurs.

Detectable differences were found in the power spectral densities of the weld

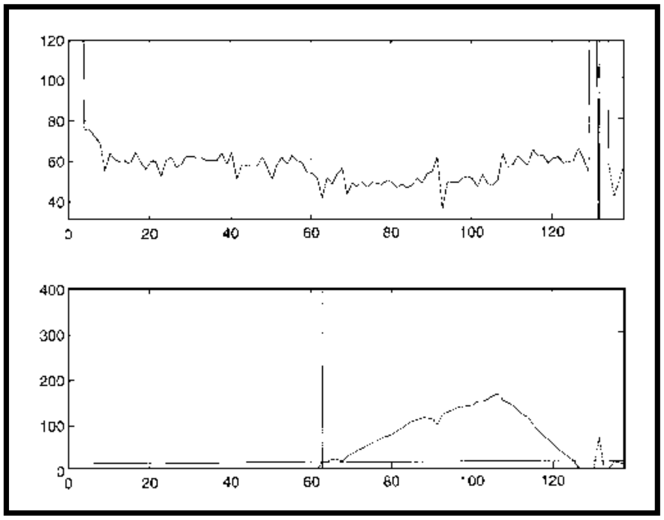

Fig. 24 — An example of the AC power waveform when spatter occurs. High voltage transients give rise to high AC power transients at 13 cm in the diagram.

voltage and current between a normal weld and welds during step disturbance (Ref. 36). The maximum spectral peak during normal welding is about 80 Hz as opposed to the maximum spectral peak during step disturbance, which is approximately 55 Hz. A detection algorithm based on the detection of changes in the fundamental frequencies, together with detection of changes in the amplitude in the fundamental frequencies shows promise. However, preliminary results described above (Ref. 36) have shown that the variance of the weld voltage is the most robust parameter for detecting changes in the weld quality.

Acknowledgments

The authors wish to express their gratitude to the Industrial Development Centre of Olofström and its personnel for their support in arranging and assisting with the experimental measurements. We also wish to acknowledge the financial support given by The Foundation for Knowledge and Competence Development (*KKS*).

References

1. Cary, H. B. 1994. *Modern Welding Technology*. Englewood Cliffs, N.J. Regents/Prentice-Hall.

2. Amin, M. 1983. Pulse current parameters for arc stability and controlled metal transfer in arc welding. *Metal Construction* 15(5): 272–278.

3. Cornu, J., and Weston, J. 1995. *Advanced Welding System,* Vol. 2, London, England, IFS.

4. Mite, T., Sakabe, A., and Yokoo, T. 1985. The estimation of arc stability of CO_2 gas shielded arc welding. *Proceedings of the Welding Institute Conference: Advanced Welding Systems*, pp. 261– 271.

5. Gupta, S. R., Gupta, P. C., and Rehfeldt, D. 1988. Process stability and spatter generation during dip transfer in MAG welding. *Welding Review*, pp. 232–241.

6. Hermans, M. J. M., and den Ouden, G. 1997. A stability criterion for short circuiting gas metal are welding. *Proceedings of the International Conference on the Joining of Materials*, Helsingør, pp. 112–119.

7. Jennings, C. 1951. Dynamic characteristics of DC welding machines. *Welding Journal* 30(2): 117–138.

8. Popkov, A., *et al.* 1977. Reducing the spatter of liquid metal in CO_2 welding by means of optimisation of the welding parameters. *Welding Production* 3: 26–27.

9. Leino, K., Nikkola, A., and Vartiainen, K. 1984. Prediction of weld defects using welding condition data. Research report 264, Technical Research Center of Finland.

10. Adam, G., and Siewert, T. A. 1990. Sensing of GMAW droplet transfer modes using an ER 100S-I electrode. *Welding Journal* 69(3): 103–108.

11. Johnson, J. A., Carlson, N. M., Smartt, H. B., and Clark, D. E. 1991. Process control of GMAW: Sensing of metal transfer mode. *Welding Journal* 70(4): 91–99.

12. Wang, W., Liu, S., and Jones, J. E. 1995. Flux cored arc welding: Arc signals, processing and metal transfer characterization. *Welding Journal* 74(11): 369– 377.

13. Ogunbiyi, B., and Norrish, A. 1996. GMAW metal transfer and arc stability assessment using monitoring indices. *Proceedings of the 6th International Conference on Computer Technology in Welding*, TWI, Cambridge, England, Abington Publishing.

14. Adolfsson, S., Ericson, K., and Agren, B. 1995. On automatic detection of burn-through in GMA welding — weld voltage analysis. Research report TULEA 1995:15, Sweden, Division of Signal Processing, Luleå University of Technology.

15. Adolfsson, S., Ericson, K., and Grennberg, A. 1996. Automatic detection of burn-through in GMA welding using a parametric model. *Mechanical Systems and Signal Processing* 10(5): 633–651.

16. Adolfsson, S., Bahrami, A., and Claesson, I. 1996. Quality monitoring in robotised welding using sequential probability ratio test. *Proceedings of TENCO '96, Digital Signal Processing Applications*, Vol. 2, New York, N.Y., IEEE. pp. 635–640.

17. Adolfsson, S., Bahrami, A., Bolmsjö, G., and Claesson, I. 1997. Automatic quality monitoring in robotised GMA welding using a repeated sequential probability ratio test method. *International Journal for the Joining of Materials* 9(1): 2–8.

18. Blakeley, P. J. 1992. Developments in monitoring systems for resistance and arc welding. *Proceedings of the International Conference on Automated Welding Systems in Manufacturing*, Paper 40. Gateshead, England, Woodhead Publishing, Ltd.

19. Agren, B. 1995, Sensor integration for robotic arc welding. Ph.D. thesis, Sweden, Lund University..

20. Hermans, M. J. M., Spikes, M. P., and den Ouden, G. 1993. Characteristic features of the short circuiting arc welding process. *Welding Review International* 12(2): 80–86.

21. Rehfeldt, D., and Schmitz, T. 1995. Investigation and measurement of weld pool oscillation in GMAW. Technical report, IIW-doc. 212-882-95.

22. Basseville, M., and Nikiforov, I.V. 1993. *Detection of Abrupt Charges: Theory and Application*. Englewood Cliffs, N.J., Prentice-Hall.

23. Grainger, R. W., Hoist, J., Isaksson, A. J., and Ninness, B. M. 1994. A parametic statistical approach to fdi for the industrial actuator benchmark. Research report LUTFD2/TFMS — 3106 — SE LUTFD2/TFMS-3106-SE, Sweden, Dept. of Mathematical Statistics, Lund Institute of Technology.

24. Lorden, G. 1971. Procedures for reacting to a change in distribution. *Ann. Math. Statistics* 42: 1897–1908.

25. Allum, C. J. 1985. Metal transfer in arc welding as a varicose instability: I. Varicose instabilities in a current-carrying liquid cylinder with surface charge. *British Journal of Applied Physics* 18(7): 1447–1468.

26. Amin, M. 1981. Synergic pulse MIG welding. *Metal Construction* 13(6): 349– 353.

27. Smith, A. A. 1966. Characteristics of the short-circuiting CO_2-shielded arc. *Physics of the Welding Arc*, Institute of Welding, pp. 75–91.

28. Lancaster, J. F., ed. 1986. *The Physics of Welding*. Oxford, England, Pergamon Press .

29. Kim, J. A., and Eager, N. M. 1991. Analysis of metal transfer in gas metal arc welding. *Welding Journal* 70(6): 91–99.

30. Mita, T., Sakabe, A., and Yokoo, T. 1988. Quantitative estimates of arc stability for CO_2 gas shielded arc welding. *Welding International* 12(2): 152–159.

31. Piuchuk, I. S., *et al.* 1980. Stabilization of transfer and methods of reducing the spattering of metal in CO_2 welding with short arc. *Automatic Welding* 6.

32. Shinoda, T, Nishikawa, H., and Shimizu, T. 1996. The development of data processing algorithms and assessment of arc stability as affected by the titanium content of GMAW wires during metal transfer. *Proceedings of the 6th International Conference on Computer Technology in Welding*, TWI, Cambridge, England, Abington Publishing, .

33. Lundin, R., and Widfeldt, M. 1988. *Mätning, registrering och övervakning av svetsdata*. Technical report 264, IVF.

34. Liu, S., and Siewert, T. 1989. Metal transfer in gas metal arc welding: droplet rate. *Welding Journal* 68(2): 52–58.

35. Lucas, W. 1985. Computers in arc welding — the next industrial revolution, part 3: instrumentation and process analysis. *Metal Construction* 17(7): 431– 436.

36. Adolfsson, S., Bahrami, A., Bolmsjö, G., and Claesson, I. 1997. Quality monitoring in robotized short circuiting GMA welding. Research report HK-R 1997:3, Sweden, Department of Signal Processing, University of Karlskrona/ Ronneby.

37. Oppenheim, A. V., and Schafer, R. W. 1989. *Discrete-Time Signal Processing*. Englewood Cliffs, N.J., Prentice-Hall.

38. Papouis, A. 1984. *Probability, Random Variables, and Stochastic Processes*. New York, N.Y., McGraw-Hill.

39. Montgomery, D. C. 1985. *Introduction to Statistical Quality Control*. New York, N.Y., J. Wiley & Sons.

40. Rao, C. R. 1973. *Linear Statistical Inference and Its Applications*. New York, N.Y.J., Wiley & Sons.

41. Wald, A. 1947. *Sequential Analysis*. New York, N.Y., J. Wiley & Sons.

42. Bagshaw, M., and Johnson, R. A. 1975. The effect of serial correlation on the performance of CUSUM-tests part II. *Technometrics* 17(1): 73–80.

43. Bagshaw, M., and Johnson, R. A. 1975. The influence of reference values and estimated variance on the ARL of the CUSUM tests. J*al Royal Statistics Society*, 37(B) (3): 413–420.

44. Bendat, J. S., and Piersol, A. G. 1986. *Random Data: Analysis and Measurement Procedures*. New York, N.Y., J. Wiley & Sons.

45. Wetherill, G. B., and Brown, D. W. 1991. *Statistical Process Control*. England, Chapman and Hall, London.

List of Symbols

α False alarm probability
f_s Sampling rate (Hz)
$g[i]$ Decision function
h Threshold for alarm
i, j, k, l, m, n Integers
I Total number of sections within a record
I Source current (A)
I_p Short-circuit peak current (A)
j Record index, instant of change
$K(m_1, m_0)$ Kullback information
$\lambda[k]$ Increment of Λ_k^j
Λ_j^k Log-likelihood ratio for observation from $y[j]$ until $y[k]$
L_i Internal inductance of the power source (H)
l_a Length of arc (mm)
l_e Length of wire electrode stickout(mm)
m Overall mean for the AC power
$m[i]$ Mean value, weld voltage, section i (V)
m_R Mean value, AC power, weld voltage, record r
m_0 Mean value, AC power, weld voltage, normal weld
m_1 Mean value, AC power, weld voltage, step disturbance
$N(0, 1)$ Normal distribution function with zero mean and unit variance
$P_{AC}[i]$ AC power of the weld voltage of section i
$P_{AC}[r, i]$ AC power of the weld voltage of the section i of the record r
$\Delta P_{AC},R[r]$ Variation between the records
$\Delta P_{AC},I[r, i]$ Variation within the record
$p_\theta(y[i])$ Probability density function
R Total number of records
R_i Internal resistance of the power source (Ω)
σ_a Standard variation of the arc time
σ_A^2 Variance of total number of reverse arrangements, A
σ_I^2 Within-record variance of the AC power
$\hat{\sigma}_I^2$ Estimated within-record variance of the AC Power
σ_R^2 Between-record variance of AC power
$\hat{\sigma}_R^2$ Estimated between-record Variance of AC power
σ_s Standard variation of the short circuit time
σ_T^2 Total variance, $\sigma_W^2 + \sigma_B^2$, of the AC power $P_{AC}[r, i]$
$\hat{\sigma}_T^2$ Estimated total variance e,$\hat{\sigma}_W^2+\hat{\sigma}_B^2$, of the AC power $P_{AC}[r, i]$
t_a Alarm instant
T Total cycle time, $T = T_a + T_{sh}$ (s)
T_a Arc time (s)
T_s Short-circuit time (s)
τ Mean delay time for detection
θ_0 Parameter before change
θ_1 Parameter after change
$u[n]$ Weld voltage at the sampling instant (V)
U_a Arc voltage (V)
U_e Wire electrode stickout voltage (V)
U_{oc} Open circuit voltage (V)
U_p Peak voltage (V)
U_w Weld voltage, $U_w = U_e + U_a$ (V)
U_{wa} Weld voltage during arc time (V)
U_{ws} Weld voltage during short-circuit time (V)
υ Change magnitude
W_b Wire melting rate (mm/s)
W_f Wire feed rate (mm/s)
W_s Welding speed (mm/s)
$y[i]$ Variance, weld voltage, section i
$y[i]$ AC power, weld voltage, section i